Radiation prevents tumor progression by inhibiting the miR-93-5p/EphA4/NF-κB pathway in triple-negative breast cancer

CHI PAN[1*], SHANSHAN SHAO[2*], YAWEN GU[2*] and QINGTAO NI[2]

Departments of [1]General Surgery and [2]Oncology, The Affiliated Taizhou People's Hospital of Nanjing Medical University, Taizhou School of Clinical Medicine, Nanjing Medical University, Taizhou, Jiangsu 225300, P.R. China

Received September 5, 2022; Accepted December 28, 2022

DOI: 10.3892/or.2023.8515

Abstract. Breast cancer (BC) is the most common type of cancer in women. Triple-negative BC (TNBC) constitutes 10-15% of all BC cases and is associated with a poor prognosis. It has previously been reported that microRNA (miR)-93-5p is dysregulated in plasma exosomes from patients with BC and that miR-93-5p improves radiosensitivity in BC cells. The present study identified EphA4 as a potential target gene of miR-93-5p and investigated the pathway related to miR-93-5p in TNBC. Cell transfection and nude mouse experiments were performed to verify the role of the miR-93-5p/EphA4/NF-κB pathway. Moreover, miR-93-5p, EphA4 and NF-κB were detected in clinical patients. The results revealed that EphA4 and NF-κB were downregulated in the miR-93-5p overexpression group. By contrast, EphA4 and NF-κB expression levels were not significantly altered in the miR-93-5p overexpression + radiation group compared with those in the radiation group. Furthermore, overexpression of miR-93-5p with concomitant radiation therapy significantly decreased the growth of TNBC tumors *in vivo*. In conclusion, the present study revealed that miR-93-5p targeted EphA4 in TNBC through the NF-κB pathway. However, radiation therapy prevented tumor progression by inhibiting the miR-93-5p/EphA4/NF-κB pathway. Therefore, it would be interesting to elucidate the role of miR-93-5p in clinical research.

Introduction

Breast cancer (BC) is the most common type of cancer in women (1). It has been estimated that ~284,200 new BC cases were diagnosed in the USA in 2022 (2). BC classification is based on molecular typing, including luminal A, luminal B, HER-2$^+$ and triple-negative BC (TNBC). Patients with luminal A BC have the best prognosis, followed by patients with luminal B BC (3). TNBC constituted 10-15% of all BC cases in the United States between 2012 and 2016 (4); however, due to the deletion of established molecular targets, patients with TNBC have a poor prognosis. Therefore, it is necessary to identify novel molecular targets for treatment. Recently, researchers have focused on the pathogenic mechanisms underlying TNBC. For example, cyclin-dependent kinase 1 (CDK1) has been reported to be highly expressed in TNBC samples (5), whereas CDK14 can act as a tumor suppressor gene in TNBC (6). Furthermore, salt-inducible kinase 2 inhibitors may decrease DNA double-strand break repair in TNBC (7). In addition, a new antibody-drug conjugate, sacituzumab govitecan, which targets trophoblast cell-surface antigen 2 was approved by the United States Food and Drug Administration (8).

The survival rate of patients with BC has increased with the discovery of novel therapeutics; however, 20-30% of patients with BC experience locoregional or distant disease recurrence worldwide (9). Radiotherapy is an integral treatment for patients with BC to promote breast-conserving surgery. Increasing the radiosensitivity of patients with BC is an effective approach to solving local recurrence. Investigating the genes associated with radiotherapy may provide additional insight into the effects of clinical radiotherapy on BC. Numerous factors are involved in radiation resistance, such as DNA repair, hypoxia and malignant behavior (10). Activating transcription factor 3 has been reported to increase radiation resistance via the PI3K/Akt signaling pathway (11). By contrast, microRNA (miRNA/miR)-142-3p decreases radiation resistance in BC (12). Moreover, miR-122 promotes cell survival in acquired radioresistant BC (13). Despite these studies, a limited number of gene markers are known to be associated with radioresistant BC and the underlying mechanism is poorly understood.

miRNAs are a group of noncoding RNAs with a small number of nucleotides (usually 20-30). miRNA inhibits target gene expression by mRNA degradation (14) and dysregulation of miRNAs has been found in numerous types of cancer (15). Our previous study revealed that miR-93-5p was upregulated

Correspondence to: Dr Qingtao Ni, Department of Oncology, The Affiliated Taizhou People's Hospital of Nanjing Medical University, Taizhou School of Clinical Medicine, Nanjing Medical University, 366 Taihu Road, Taizhou, Jiangsu 225300, P.R. China
E-mail: nqt1990@126.com

*Contributed equally

Key words: microRNA-93-5p, EphA4, NF-κB, radiosensitivity, triple-negative breast cancer

in plasma exosomes from patients with BC (16). A further study revealed that miR-93-5p improved the sensitivity of BC cells to radiation (17). Given the unknown underlying mechanism, the present study aimed to identify the related miR-93-5p pathway for patients with TNBC in clinical and *in vivo* settings. The experimental design is summarized in Fig. 1.

Materials and methods

Database analysis. The miR-93-5p target gene was identified using three well-known bioinformatics prediction algorithms: TargetScan (https://www.targetscan.org/vert_71/), microRNA (http://cbio.mskcc.org/miRNA2003/miranda.html and miRDB (http://www.mirdb.org/miRDB). The starBase database (http://starbase.sysu.edu.cn) was used to identify the potential target sequences of miR-93-5p and EphA4. The expression of miR-93-5p was analyzed in 1,085 breast cancer and 104 normal samples from healthy individuals. The expression of EphA4 and NF-κB was analyzed in 1,104 cancer and 113 normal samples. The expression data of genes in cancer were downloaded from The Cancer Genome Atlas project via the Genomic Data Commons Data Portal (https://portal.gdc.cancer.gov/). The starBase database was also employed to assess the correlations between miR-93-5p expression and EphA4/NF-κB expression.

Cell culture and transduction. The MDA-MB-231 cell line (cat. no. MXC234) was purchased from The Cell Bank of Type Culture Collection of The Chinese Academy of Sciences. This cell line was cultured in RPMI 1640 (Corning, Inc.) medium containing 10% fetal bovine serum (FBS; Gibco; Thermo Fisher Scientific, Inc.), 100 U/ml penicillin and 100 μg/ml streptomycin. MCF-7 cells (HTB-22; American Type Culture Collection) were cultured in Dulbecco's modified Eagle's medium (Cytiva) supplemented with 10% FBS, 100 U/ml penicillin and 100 μg/ml streptomycin. The cells were cultured in an atmosphere containing 5% CO_2 at 37˚C.

The 2nd generation system was used to package lentiviruses. To induce transient expression of miR-93-5p' (5'-CTG GGGGCTCCAAAGTGCTGTTCGTGCAGGTAGTGTGA TTACCCAACCTACTGCTGAGCTAGCACTTCCCGAGC CCCCGG-3'; Quanyang) the cloning vector (pCDH-CMV-MCS-EGFP-EF1-Puro; Quanyang) was constructed using *Bam*HI (cat. no. NEB R0136) and *Eco*RI (cat. no. NEB R0101) restriction enzymes (both from New England BioLabs, Inc.). The lentiviral plasmid (5 μg; 1 μg/μl) (3.75 μg pH1 packaging plasmid and 1.25 μg pH2 envelope packaging plasmid; Beijing Yingmao Shengye Biotechnology Co., Ltd.) was transfected into 293T (cat. no. MXC006; Shanghai Meixuan Biotechnology Co.) cells using Lipofectamine® 2000 reagent (Invitrogen; Thermo Fisher Scientific, Inc.) at 37˚C for 4 h. The viral supernatant was collected, filtered and concentrated by ultracentrifugation (80,000 x g, 4˚C, 2 h) after a 48-h incubation with new culture medium. MDA-MB-231 cells with stable overexpression (OE) of miR-93-5p were established by lentiviral infection. MDA-MB-231 cells were infected with lentivirus at a MOI of 10 with polybrene at 37˚C for 24 h. Puromycin (2 μg/ml) was used to select a stable cell line. MDA-MB-231 cells were also infected with the empty lentiviral vector as negative control.

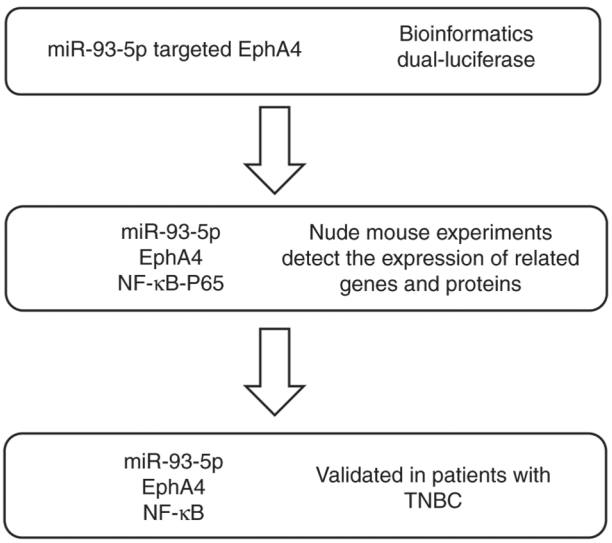

Figure 1. Flow diagram of the experimental design. miR-93-5p, microRNA-93-5p; TNCB, triple-negative breast cancer.

Table I. List of primers used for reverse transcription-quantitative PCR.

Gene name	Sequence, 5'-3'
miR-93-5p	F: GCGCCAAAGTGCTGTTCGTGC
	R: TGCAGGGTCCGAGGTAT
U6	F: CTCGCTTCGGCAGCACA
	R: AACGCTTCACGAATTTGCGT
EphA4	F: CTGTTCAGGGAGAGCTTGGG
	R: CCTTGTCGTTGTCCGACTCA
NF-κB	F: GCAGGAACTCAAGGGAGCTAA
	R: TCCACGAACTGGCTGTTGAG
GAPDH	F: GACAGCCGCATCTTCTTGTG
	R: AATCCGTTCACACCGACCTT

F, forward; miR-93-5p, microRNA-93-5p; R, reverse.

RNA extraction and reverse transcription-quantitative PCR (RT-qPCR). RNAiso PULS (Takara Bio, Inc.) was used to isolate total RNA from MDA-MB-231 cells and TNBC tissues. One-step RT-qPCR was performed using SYBR Premix Ex Taq (Takara Bio, Inc.) and a CFX 96 System (Bio-Rad Laboratories, Inc.). The RT-qPCR thermal cycling conditions were as follows: 50˚C for 10 min and 95˚C for 5 min, followed by 40 cycles at 95˚C for 15 sec and 60˚C for 30 sec. The dissociation stage (95˚C for 15 sec, 60˚C for 1 min and 95˚C for 15 sec) was performed after amplification. U6 was used as an internal control for miRNA expression. The sequences of primers used in the present study are listed in Table I. The standard $2^{-\Delta\Delta Cq}$ method was used to calculate relative RNA abundance (18).

Luciferase assay. Wild-type (WT) or mutant (Mut) EphA4 was amplified and cloned into a pmirGLO (Beyotime Institute of Biotechnology) vector. Due to the poor survival

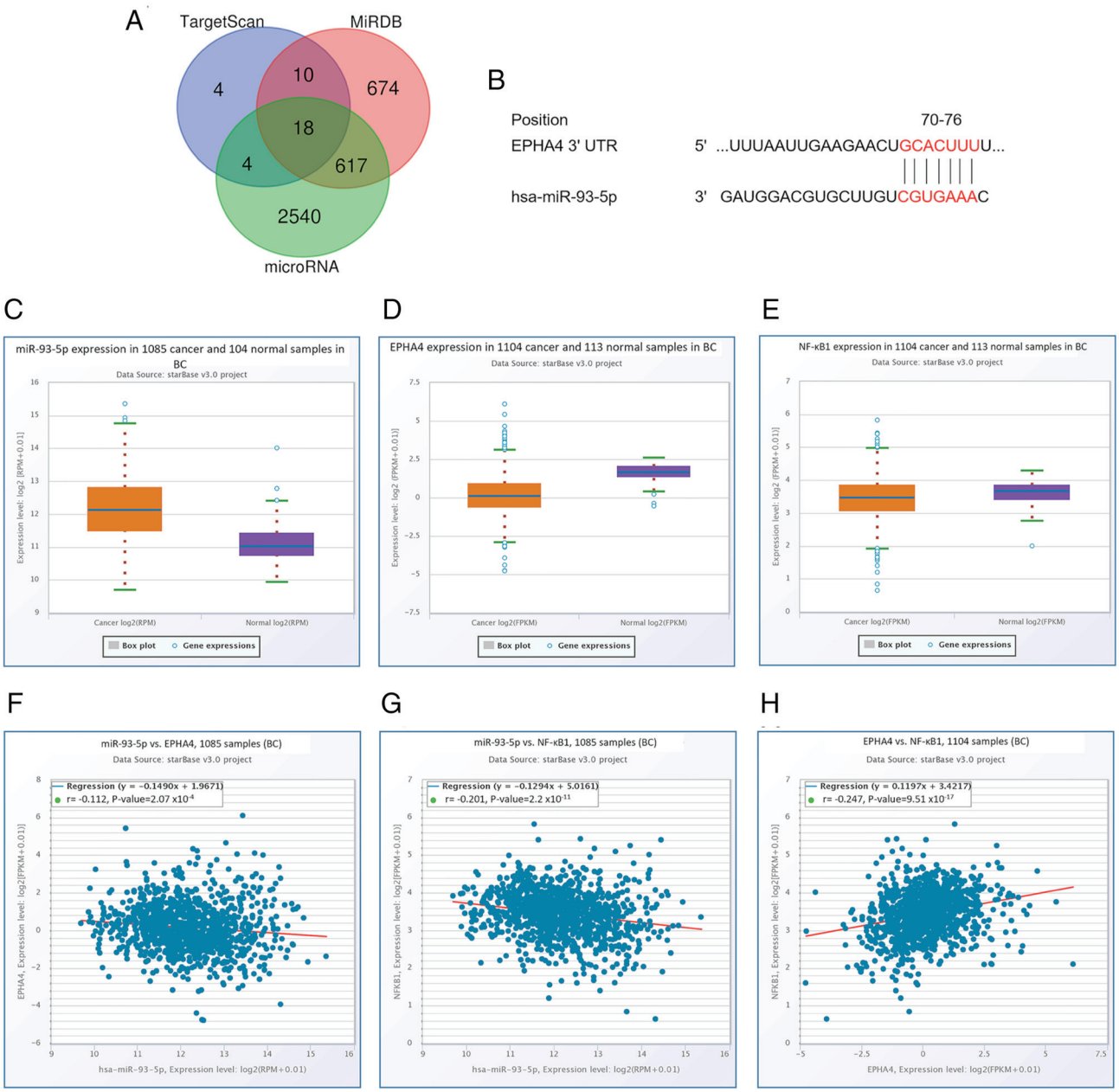

Figure 2. (A) Venn diagram of the predicted target genes of miR-93-5p. (B) EphA4 is a putative target gene of miR-93-5p. (C) miR-93-5p was highly expressed in BC samples in starBase. (D) EphA4 was downregulated in BC samples in starBase. (E) NF-κB1 was downregulated in BC samples in starBase. (F) miR-93-5p expression was negatively correlated with that of EphA4 in starBase. (G) miR-93-5p expression was negatively correlated with that of NF-κB1 in starBase. (H) EphA4 expression was positively correlated with that of NF-κB1 in starBase. BC, breast cancer; miR-93-5p, microRNA-93-5p.

of MDA-MB-231 cells post-transduction, the luciferase assay was only performed in MCF-7 cells. MCF-7 cells ($2x10^5$) were seeded in 96-well plates and were co-transfected with miR-93-5p mimic or miR-negative control (NC) and EphA4 WT or Mut plasmids, using Lipofectamine 3000 (Invitrogen; Thermo Fisher Scientific, Inc.), according to the manufacturer's instructions. The miR mimic sequences were as follows: Hsa-miR-93-5p mimic, sense 5'-CAAAGU GCUGUUCGUGCAGGUAG-3', anti-sense 5'-ACCUGCACG AACAGCACUUUGUU-3'; miR-NC (nonspecific scrambled RNA), sense 5'-UUCUCCGAACGUGUCACGUTT-3' and anti-sense 5'-ACGUGACACGUUCGGAGAATT-3'. Cells were harvested 48 h after transfection. Finally, the luciferase activity was measured using a Dual-Luciferase Reporter Assay System (Promega Corporation). Using the *Renilla* luciferase as an internal control, the relative luciferase activity is presented as a ratio of firefly luciferase intensity to *Renilla* luciferase intensity.

Tumor xenograft model. MDA-MB-231 cells ($5x10^7$) with or without miR-93-5p OE were injected subcutaneously into 4-week-old BALB/c female mice. All BALB/c nude mice (weight, 18±2 g) were purchased from Silaike Laboratory Animal Co., Ltd. A total of 24 mice were randomly divided into the following four groups (n=6 rats/group: negative control; miR-93-5p OE; radiation therapy (RT) and miR-93-5p OE + RT groups. All mice were housed in a specific pathogen-free sterile environment with a constant temperature

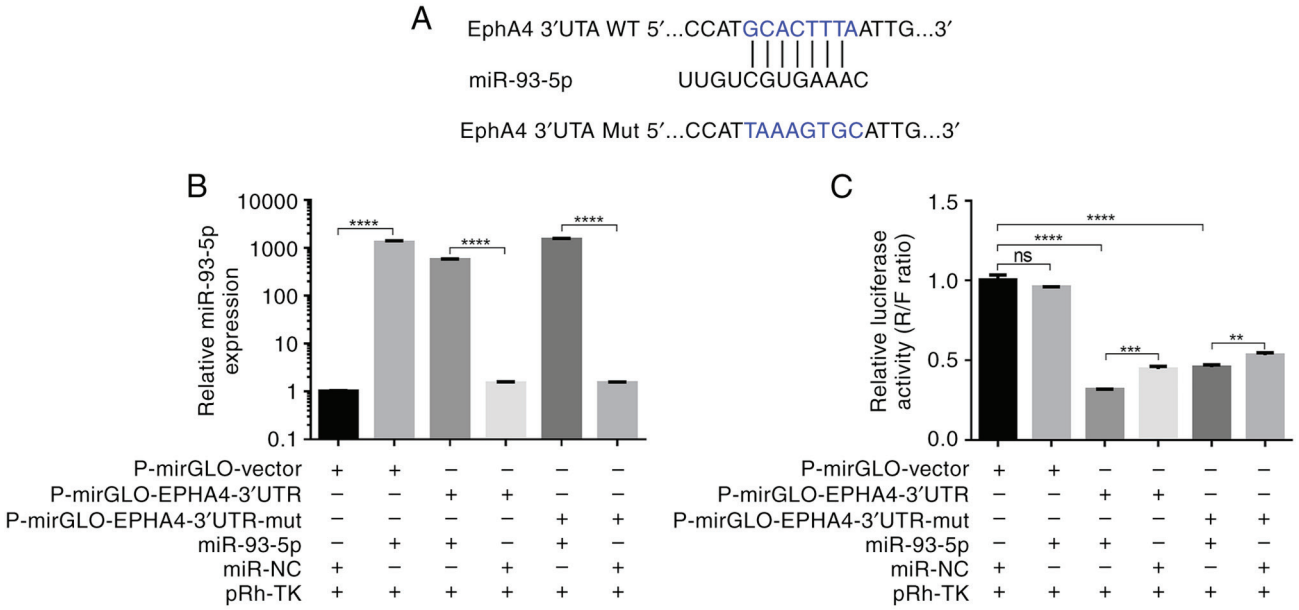

Figure 3. (A) Schematic representation of the seed region between miR-93-5p and the WT and Mut sequences of EphA4 3'-UTR. (B) miR-93-5p expression was significantly upregulated in cells transfected with miR-93-5p mimic. (C) miR-93-5p suppressed the luciferase activity of WT and Mut EphA4 3'-UTR. Data are expressed as the mean ± SD of three independent experiments. **P<0.01, ***P≤0.001, ****P≤0.0001. miR-93-5p, microRNA-93-5p; Mut, mutant; NC, negative control; R/F, *Renilla*/firefly; WT, wild-type.

of 25˚C, under a 12-h light/dark cycle, a relative humidity of 50-70%, with free access to adequate food and water supply. Mice were acclimated for 1 week before tumor injection and tumors of ~1 mm in size were felt ~1 week after inoculation. The body weights of the mice were measured every 3 days. The NC (negative control) group mice were injected by MDA-MB-231 cells transfected with an empty vector with a lentivirus. In the RT and miR-93-5p OE + RT groups, 4 Gy RT was administered three times in 1 week on days 1, 4 and 7 and began when the tumor diameter was 5-7 mm (16 days after injection). The mice were sacrificed by cervical dislocation on the next day after the third irradiation. The humane endpoint was determined as a tumor volume of 1 cm^3 and no animals reached the humane endpoint in the present study. All mice were humanely sacrificed 4 weeks after tumor injection. Death was verified by the cessation of breathing and heartbeat. After the mice were sacrificed, the maximum (L) and minimum (W) lengths and weights of tumors were determined. The tumor volume was estimated to be (L x W x W)/2. Hematoxylin and eosin (H&E) staining was performed to evaluate tissue morphology. Animal ethics approval was obtained from the Medical College of Yangzhou University of Animal Ethics Committee (approval no. YXYLL-2021-64).

Pathological section analysis. The collected mouse tumor tissues were fixed in 4% paraformaldehyde for 24 h at room temperature, dehydrated, and immersed in paraffin. Subsequently, 4 μm sections were cut on a glass slide using a Leica RM2145 microtome (Leica Microsystems, Ltd.) and allowed to dry at 40˚C for 2 h before staining. Xylene was used to dewax the slides and ethanol was used to rehydrate the slides. H&E staining was performed for 5 min in Mayer's hematoxylin and for 2 min in eosin at room temperature. Images of the slides were captured using a Cewei LW300LFT LED light microscope with a maximum magnification of x200. H&E staining was used to observe pathological damage under a microscope.

Western blotting. Proteins were extracted from MDA-MB-231 cells using RIPA lysis buffer (Beyotime Institute of Biotechnology) and protein concentration was determined using a BCA Kit (Beyotime Institute of Biotechnology). Proteins (20 μg) were separated by SDS-PAGE on 12% gels and were then transferred to 0.45 μm PVDF membranes (MilliporeSigma). The membranes were blocked with 5% skim milk powder for 2 h at room temperature and incubated overnight at 4˚C with the following primary antibodies: EphA4 1:1,000; cat. no. A8346; ABclonal Biotech Co., Ltd.), NF-κB (1:1,000; cat. no. 8242T; Cell Signaling Technology, Inc.), GAPDH (1:5,000; cat. no. 5174; Cell Signaling Technology, Inc.). The membranes were then incubated with a HRP-conjugated goat anti-rabbit IgG secondary antibody (1:5,000; cat. no. 111-035-003; Jackson ImmunoResearch Laboratories, Inc.) at room temperature for 2 h, and the protein bands were detected using an ECL detection system (Bio-Rad Laboratories, Inc.). GAPDH was used as a control. The relative expression levels were calculated as follows: (band intensity of target protein/band intensity of control protein); this was measured using Image-Pro Plus 6.0 software (Media Cybernetics, Inc.).

Patients and clinical parameters. This prospective study investigated 43 TNBC formalin-fixed and paraffin-embedded (FFPE) samples and normal adjacent tissue (≥0.5 cm away from TNBC tissues) from patients who underwent surgery between January 2018 and March 2021 at the Jiangsu Taizhou People's Hospital (Taizhou, China). FFPE samples were fixed in 4% paraformaldehyde for 24 h at room temperature, dehydrated

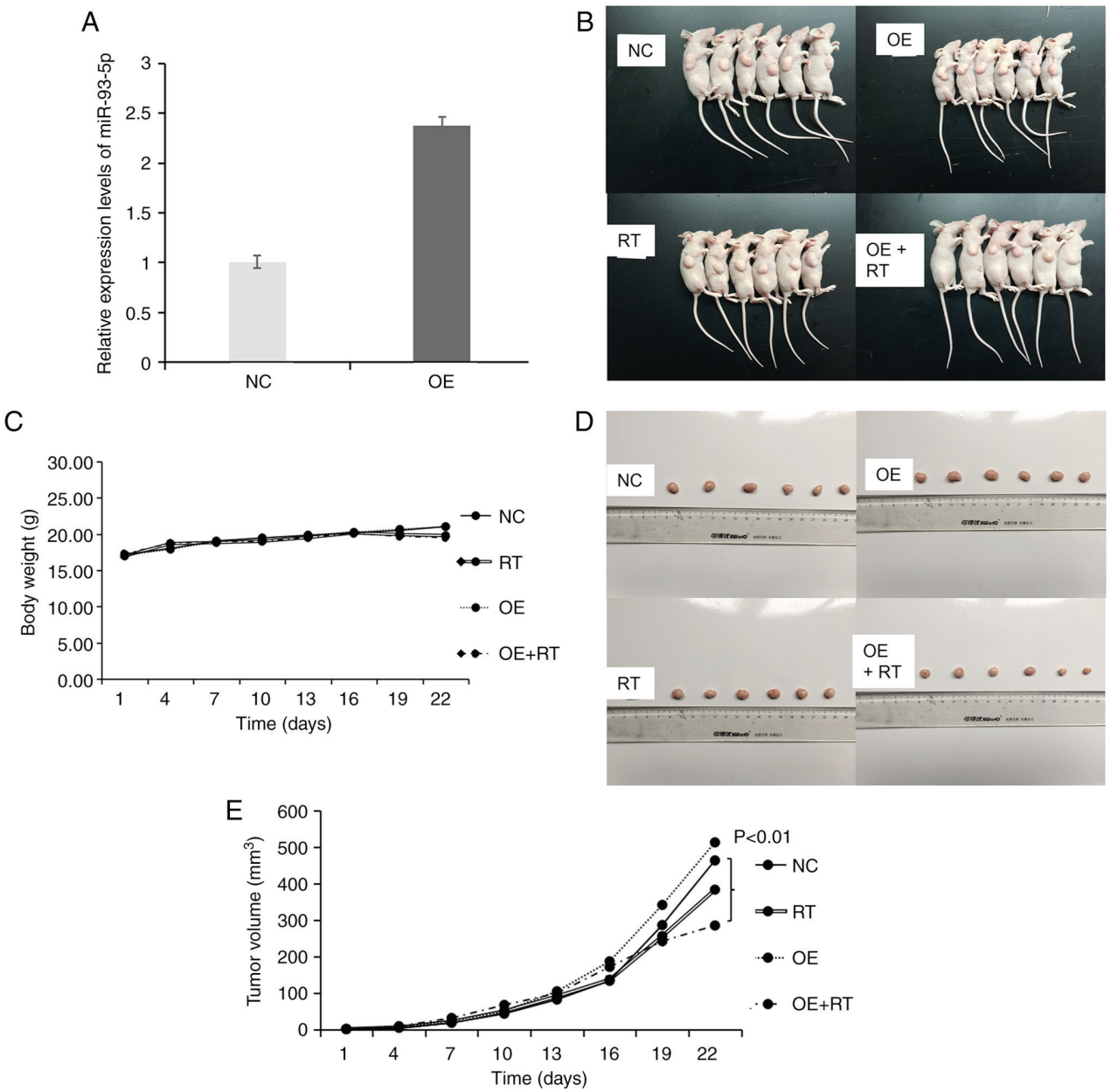

Figure 4. (A) miR-93-5p expression was significantly upregulated in the OE group. (B) Digital images of nude mice with xenograft triple negative breast cancer. (C) Body weight of each group of nude mice showed no significant difference between the groups. (D) Maximum diameter of xenograft tumors. (E) Changes in tumor volume in the xenograft mice. miR-93-5p, microRNA-93-5p; NC, negative control; OE, overexpression; RT, radiation therapy.

and embedded in paraffin and cut into 10 μm sections. None of the patients had received RT or chemotherapy before surgery. The mean age was 53.02 years (age range, 29-74 years), and the patients neither drank nor smoked. At the time of diagnosis, the current TNM status of each patient was classified according to the American Joint Committee on Cancer 8th edition (19). The Human Ethics Review Committee of Jiangsu Taizhou People's Hospital approved the present study (approval no. KY 2021-043-01). The requirement for informed consent was waived by the Human Ethics Review Committee of Jiangsu Taizhou People's Hospital.

RNA extraction. FFPE sections were sliced to a thickness of 10 μm for subsequent RT-qPCR experiments. Finally, total RNA was extracted from FFPE using the mRNA prep Pure FFPE Kit (cat. no. DP502; Tiangen Biotech Co., Ltd.) according to the instructions provided by the manufacturer.

Statistical analysis. The present study investigated the relationships between miR-93/EphA4/NF-κB expression and clinicopathological characteristics using Spearman's correlation analysis and χ^2 test. The mean ± SD of three separate experiments were used to calculate all data. Differences between two groups were assessed using an unpaired Student's t-test, and between paired variables were assessed using a paired Student's t-test. Multiple group comparisons were assessed using one-way ANOVA followed by Bonferroni test to determine significance. P<0.05 was considered to indicate a statistically significant difference. SPSS version 18.0 (SPSS, Inc.) was used for all statistical analyses.

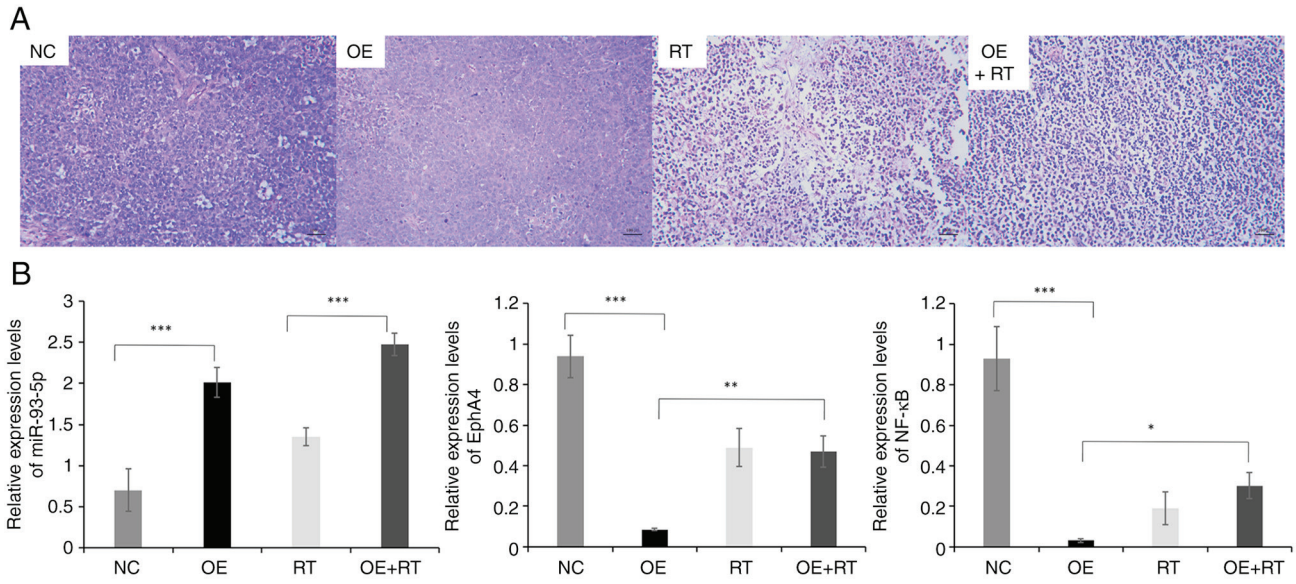

Figure 5. (A) Hematoxylin and eosin-stained images of each group (magnification, x200). (B) Expression levels of miR-93-5p, EphA4 and NF-κB-P65 detected by reverse transcription-quantitative PCR. Results are presented as the mean ± SD. *P<.05, **P<0.01, ***P≤0.001. miR-93-5p, microRNA-93-5p; NC, negative control; OE, overexpression; RT, radiation therapy.

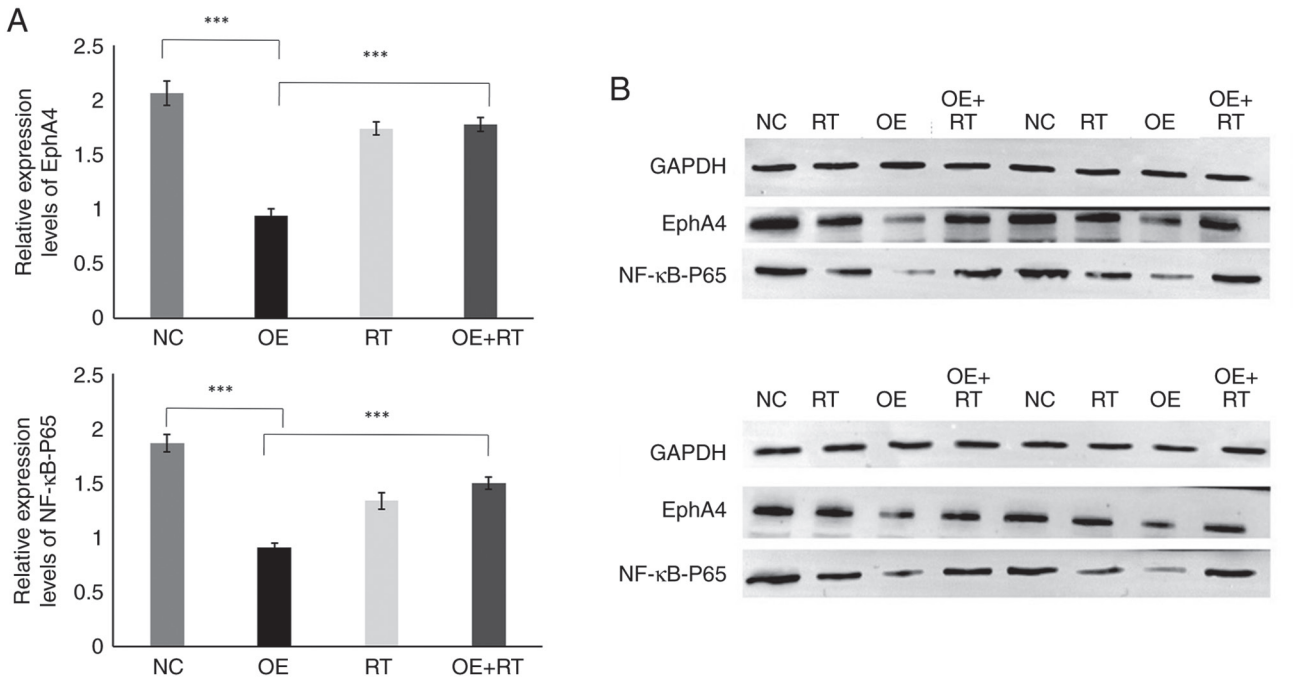

Figure 6. (A) Semi-quantification of western blotting. (B) Expression levels of EphA4 and NF-κB-P65 were detected by western blotting. Results are presented as the mean ± SD. ***P≤0.001. NC, negative control; OE, overexpression; RT, radiation therapy.

Results

miR-93-5p directly targets EphA4 3'-UTR. The miR-93-5p target gene was identified using three well-known bioinformatics prediction algorithms: TargetScan, microRNA and miRDB. Based on the results, 18 genes were predicted to be miR-93-5p candidates (Fig. 2A). EphA4 was one of the genes that was considered a potential target for miR-93-5p (Fig. 2B). The online bioinformatics tool starBase demonstrated that miR-93-5p expression was significantly higher in BC samples compared with those in normal controls (P<0.001; Fig. 2C), whereas EphA4 expression was significantly lower (P<0.001; Fig. 2D). The expression levels of NF-κB were also low in BC samples (P<0.01; Fig. 2E). In addition, a significant negative correlation was identified between miR-93-5p and EphA4 expression (P<0.001; Fig. 2F), and the expression of miR-93-5p was negatively correlated with NF-κB (P<0.001; Fig. 2G), whereas a positive correlation was identified between EphA4 and NF-κB (P<0.001; Fig. 2H); however, all correlations were weak (r-values were <0.3/-0.3).

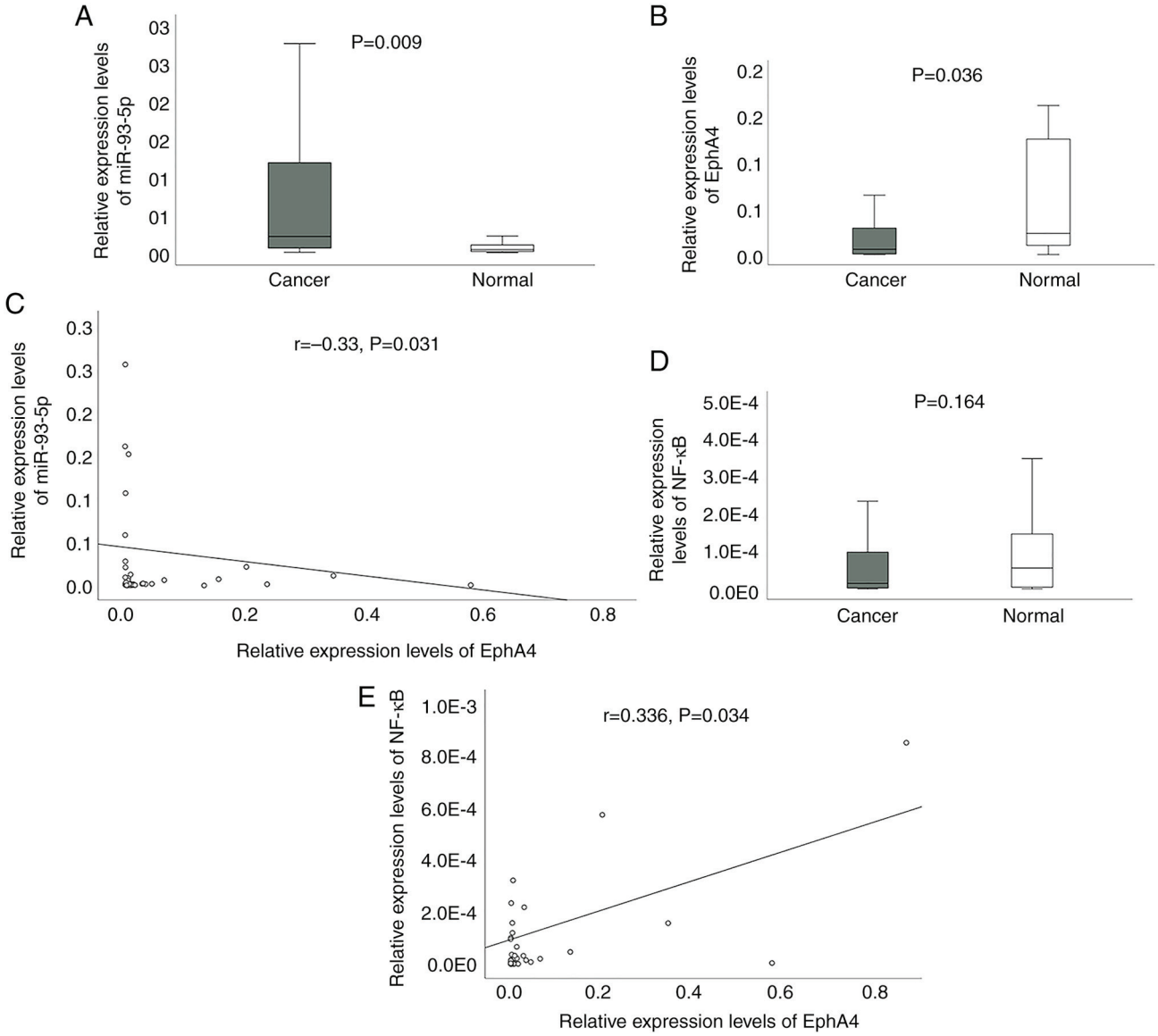

Figure 7. Relative expression levels of (A) miR-93-5p and (B) EphA4 in patient tissues. (C) An inverse correlation between miR-93-5p and EphA4 was detected by RT-qPCR. (D) Relative expression levels of NF-κB in patient tissues was detected by RT-qPCR. (E) A positive correlation was detected between NF-κB and EphA4. Results are presented as the mean ± SD. miR-93-5p, microRNA-93-5p; RT-qPCR, reverse transcription-quantitative PCR.

Luciferase reporter vectors containing WT and Mut EphA4 3'-UTRs were generated to further validate the interaction between miR-93-5p and EphA4 (Fig. 3A). A dual-luciferase reporter assay confirmed that miR-93-5p can directly bind to the EphA4 3'-UTR. Transfection of MCF-7 cells with miR-93-5p mimic or miR-NC revealed that cells transfected with the miR-93-5p mimic had significantly increased miR-93-5p expression (miR-93-5p vs. miR-NC; miR-93-5p + EphA4 vs. miR-NC + EphA4; miR-93-5p + EphA4-Mut vs. miR-NC + EphA4-Mut; P<0.0001; Fig. 3B). When miR-93-5p and the p-mirGLO-EphA4-3'UTR were co-transfected into MCF-7 cells, the luciferase signal was significantly lower than that in cells transfected with miR-NC (P<0.001; Fig. 3C). In addition, miR-93-5p suppressed luciferase activity when co-transfected with a luciferase reporter containing Mut EphA4 3'-UTR (Fig. 3C). These findings indicated that the predicted binding site and the designed Mut EphA4 were not suitable. However, it still can be seen that the strength of the binding site in Mut EphA4 3'-UTR was weaker than that in WT EphA4 3'-UTR. These findings indicated that miR-93-5p directly targets the EphA4 3'-UTR.

miR-93-5p OE improves the radiosensitivity of MDA-MB-231 cells to RT in vivo. Our previous study reported that miR-93-5p could improve the radiosensitivity of MDA-MB-231 cells (17); therefore, animal experiments were performed to validate the role of miR-93-5p *in vivo*. First, miR-93-5p OE vectors were constructed. RT-qPCR confirmed that miR-93-5p was overexpressed in the MDA-MB-231 OE group (Fig. 4A). Subsequently, experiments with tumor xenografts were conducted to examine whether miR-93-5p OE rendered TNBC tumors more susceptible to RT *in vivo* (Fig. 4B). Notably, the body weight of the tumor-bearing nude mice in each group was not significantly different (Fig. 4C). Xenograft tumor weights were measured after the nude mice were sacrificed (Fig. 4D). Comparing tumor sizes revealed that the OE of miR-93-5p in

Table II. Clinicopathologic associations of miR-93-5p, EphA4 and NF-κB expression in triple-negative breast cancer (n=43).

Clinical characteristic	Total number	miR-93-5p, n	EphA4, n	NF-κB, n
Age, years				
≤50	16	16	16	15
>50	27	27	27	25
P-value		0.31	0.37	0.908
Tumor size				
≤2 cm (T1)	17	17	17	15
>2 cm (T2-T3)	26	26	26	25
P-value		0.442	0.549	0.0498
Lymph node metastasis				
0 (N0)	29	29	29	26
≥1 (N1-N3)	14	14	14	14
P-value		0.049	0.901	0.206
Stage				
I	15	15	15	13
II-III	28	28	28	27
P-value		0.375	0.396	0.0498
Ki67				
<50%	13	13	13	12
≥50%	30	30	30	28
P-value		0.444	0.349	0.425

miR-93-5p, microRNA-93-5p. The patients were divided into two subgroups according to each variable and the number of cases in each subgroup is shown. The expression levels of miR-93-5p, EphA4 and NF-κB in two groups (e.g., expression in ≤50 group vs. expression in >50 group) were compared using independent samples t-test and the resultant P-values were obtained.

the MDA-MB-231 cells used to generate xenografts combined with concurrent RT significantly reduced tumor formation compared with that in the NC group (P<0.01; Fig. 4E).

The H&E-stained images are shown in Fig. 5A. H&E staining revealed that the tumor cells in the NC and OE groups grew well, with large and round cell nuclei. Dividing cells and abundant microvessels were also observed in the NC and OE groups. Distinct shrinkage of the cytoplasm, wrinkled cell nuclei, some lysed nuclei and a large necrotic area were visible in the RT group. Furthermore, necrosis in the OE + RT group was much more severe than in RT group.

To further understand the mechanisms underlying the effects of miR-93-5p, downstream regulatory genes were progressively explored. Based on the bioinformatics analysis, it was hypothesized that miR-93-5p targeting EphA4/NF-κB could improve the effects of RT on TNBC cells. The expression levels of miR-93-5p, EphA4 and NF-κB in each group (three tumors/group) are displayed in Fig. 5B. EphA4 and NF-κB expression levels were decreased in the miR-93-5p OE group compared with those in the NC group (P<0.001). Moreover, the expression levels of EphA4 and NF-κB were increased in the miR-93-5p OE + RT group compared with those in the OE group (P<0.001). However, the expression levels of EphA4 and NF-κB were not significantly different between the RT and OE + RT groups. In addition, western blotting was performed and the blots were semi-quantified (Fig. 6A and B). The relative expression levels of EphA4 and NF-κB were significantly lower in the miR-93-5p OE group compared with those in the NC group (P<0.001). Moreover, the relative expression levels of EphA4 and NF-κB were higher in the miR-93-5p OE + RT group compared with those in the OE group (P<0.001). Similar to the RT-qPCR results, the relative expression levels of EphA4 and NF-κB were not significantly different between the RT and OE + RT groups. These findings indicated that RT may prevent the miR-93-5p/EphA4/NF-κB pathway.

miRNA-93-5p is downregulated in patients with TNBC. RT-qPCR was used to evaluate the expression levels of miR-93-5p, EphA4 and NF-κB in 43 pairs of TNBC and adjacent tissues. The clinicopathological associations between miR-93-5p, EphA4 and NF-κB expression in TNBC are presented in Table II. Notably, the expression levels of miR-93-5p were lower in patients with TNBC with positive lymph nodes (P=0.049). NF-κB expression was higher in patients with a larger tumor size (P=0.049) and later TNM stage (P=0.0498). miR-93-5p expression was upregulated (P=0.009), whereas EphA4 was downregulated in TNBC (P=0.036) (Fig. 7A and B). Correlations between expression levels were determined using the Spearman's test. The analysis revealed an inverse relationship (r=-0.33, P=0.031) between miR-93-5p and EphA4 (Fig. 7C). Although NF-κB expression did not differ between normal and cancerous tissues (P=0.164; Fig. 7D), a positive correlation was identified between NF-κB and EphA4 expression (r=0.336, P=0.034; Fig. 7E). The correlation analysis also found no significant differences between miR-93-5p and NF-κB (data not shown).

Discussion

TNBC is a fatal subtype of BC, with a high proclivity for distant metastases and few therapeutic choices (20). At present, the overall survival of patients with TNBC remains poor. Recently, targeted cancer therapy has attracted the attention of a number of researchers. Strictinin is a targeted ROR1 inhibitor that may decrease the proliferation of TNBC (21). Clofazimine reduces TNBC growth by targeting the Wnt signaling pathway (22). However, available biomarkers cannot deliver the desired effect in terms of diagnosis and prognosis in patients with TNBC. Thus, identifying novel molecular markers and therapeutic targets is critical for reducing the recurrence and mortality of TNBC.

miRNAs have been regarded as potential oncogenes and tumor suppressors in numerous types of cancer. In a previous study, miR-93-5p was shown to be dysregulated in exosomes from patients with BC (16). A single miRNA can regulate various target genes. Sun *et al* (23) determined that miR-93-5p could promote the progression of cervical cancer by targeting the THBS2/MMPs signaling pathway. Wu *et al* (24) reported that miR-93-5p could inhibit glioma cell proliferation and metastasis by targeting MMP2. Wang *et al* (25) demonstrated that miR-93-5p increased the apoptosis and adriamycin resistance of BC cells by inhibiting the expression of Bcl-2 and

P-GP protein. In the present study, bioinformatics analysis was used to identify the target gene of miR-93-5p. A dual-luciferase reporter experiment confirmed that EphA4 was a candidate target gene of miR-93-5p. However, the luciferase reporter also showed miR-93-5p suppressed Mut EphA4 3'-UTR. The strength of the binding site in Mut EphA4 3'-UTR was weaker than that in WT EphA4 3'-UTR. These findings indicated that a limitation of the present study may be that the predicted binding site of Mut EphA4 may not be suitable. Additional unknown binding sites may exist between mut-EphA4 and miR-93-5p. In future, experiments should be designed with shorter gene fragments for mut-EphA4 to avoid interference from other sequences.

Eph is the largest branch of the receptor tyrosine kinases family (26). EphA4 is the only Eph family member that can bind to ephrin-A and ephrin-B ligands (27). EphA4 is mainly involved in nervous system disorders and cancer development (28). A previous study on the nervous system revealed that treatment targeting EphA4 could improve ischemic stroke (29). miR-93 has also been reported to promote neurite growth of spinal cord neurons by targeting EphA4 (30). In addition, treatment targeting EphA4 can eliminate the chemoresistance of cervical cancer cells (31), and EphA4 has been shown to be associated with the failure of RT for rectal cancer (32). Moreover, the aggressive phenotype of colorectal cancer cells that have endured RT is controlled by EphA4-mediated signaling (33). EphA4 deficiency has been linked to high grade, advanced TNM stage, lymph node metastases and a poor prognosis in BC (34). Moreover, a previous study reported that miR-335 can inhibit EphA4 in BC to suppress its progression (35).

The radiosensitivity of cancer cells is a major factor in determining the effectiveness of cancer RT. Radiosensitivity is a multi-gene, intricate process with an unclear mechanism. Zheng *et al* (36) reported that Linc-RA1 was upregulated in radioresistant glioma cells and promoted glioma radioresistance *in vitro* and *in vivo*. In our previous study, it was revealed that miR-93-5p increased the radiosensitivity of TNBC cells (17). To further investigate the underlying mechanisms, the present study transfected MDA-MB-231 cells with a miR-93-5p mimic and used this cell line to generate a tumor xenograft model. NF-κB is a transcription factor that was found in the nuclear extract of B lymphocytes in 1986 (37). NF-κB is closely connected to various activities, including tumor initiation, development and metastasis, and the NF-κB pathway is critical for tumor cell development and radiation resistance (38). In the present study, the difference in NF-κB expression in patients with TNBC with a large tumor size or in the later stages of TNBC were only of borderline significance. The borderline significant findings may be related to the small sample size. Lu *et al* (39) reported that EphA4 activates NF-κB and induces BC stem cells to secrete various cytokines to maintain stem cell status. The present study also detected changes in EphA4 and NF-κB. In cancer tissue, miR-93-5p expression was increased, whereas EphA4 expression was decreased. Additionally, a negative correlation between EphA4 expression and miR-93-5p expression was identified in clinical samples. In animal experiments, a decrease in EphA4 and NF-κB expression was detected in the miR-93-5p OE group. These findings indicated that miR-93-5p may regulate EphA4 and NF-κB. However, miR-93-5p OE in the MDA-MB-231 cells used to generate the xenografts and the treatment of mice with RT significantly decreased tumor development. This result confirmed our previous results, which revealed that miR-93-5p increased the radiosensitivity of BC *in vitro* (17). Moreover, EphA4 and NF-κB expression levels in the miR-93-5p OE + RT group were not significantly different compared with those in the RT group, but they were increased compared with in the miR-93-5p OE group. These results indicated that RT may prevent tumor progression by inhibiting the miR-93-5p/EphA4/NF-κB pathway. The findings of the present study, alongside those of previous studies, indicated that RT may affect gene expression, with miR-93-5p interacting with RT and altering its effect. RT was shown to block the binding sites between miR-93-5p and EphA4, which increased the expression levels of miR-93-5p and had subsequent effects on EphA4 and NF-kB. However, the potential mechanisms have not yet been fully elucidated and require further investigation.

In conclusion, the present study revealed that miR-93-5p targeted EphA4 in TNBC through the NF-κB pathway. However, RT prevented tumor progression by inhibiting this pathway. Therefore, future clinical studies should aim to elucidate the role of miR-93-5p.

Acknowledgements

Not applicable.

Funding

This work was supported by the Jiangsu Provincial Double-Innovation Doctor Program (grant nos. 202030205 and 202030206).

Availability of data and materials

The datasets used and/or analyzed during the current study are available from the corresponding author on reasonable request.

Authors' contributions

All of the authors contributed to the conception and design of the study. QN and SS performed the experimental operation, and data were collected by YG. The experimental design and data analysis were performed by CP. The first draft of the manuscript was written by QN, and all the authors commented on the previous versions. QN and CP confirm the authenticity of all the raw data. All authors have read and approved the final manuscript.

Ethics approval and consent to participate

The Human Ethics Review Committee of Jiangsu Taizhou People's Hospital approved the present study (approval no. KY 2021-043-01). The requirement for informed consent was waived by the Human Ethics Review Committee of Jiangsu Taizhou People's Hospital.

Patient consent for publication

Not applicable.

Competing interests

The authors declare that they have no competing interests.

References

1. Liang Y, Song X, Li Y, Chen B, Zhao W, Wang L, Zhang H, Liu Y, Han D, Zhang N, *et al*: LncRNA BCRT1 promotes breast cancer progression by targeting miR-1303/PTBP3 axis. Mol Cancer 19: 85, 2020.
2. Siegel RL, Miller KD, Fuchs HE and Jemal A: Cancer statistics, 2022. CA Cancer J Clin 72: 7-33, 2022.
3. Gao JJ and Swain SM: Luminal A breast cancer and molecular assays: A review. Oncologist 23: 556-565, 2018.
4. DeSantis CE, Ma J, Gaudet MM, Newman LA, Miller KD, Goding Sauer A, Jemal A and Siegel RL: Breast cancer statistics, 2019. CA Cancer J Clin 69: 438-451, 2019.
5. Pan C, Cong A and Ni Q: Microarray data reveal potential genes that regulate triple-negative breast cancer. J Int Med Res 50: 3000605221130188, 2022.
6. Zhang M, Zhang L, Geng A, Li X, Zhou Y, Xu L, Zeng YA, Li J and Cai C: CDK14 inhibition reduces mammary stem cell activity and suppresses triple negative breast cancer progression. Cell Rep 40: 111331, 2022.
7. Lu Z, Mao W, Yang H, Santiago-O'Farrill JM, Rask PJ, Mondal J, Chen H, Ivan C, Liu X, Liu CG, *et al*: SIK2 inhibition enhances PARP inhibitor activity synergistically in ovarian and triple-negative breast cancers. J Clin Invest 132: e146471, 2022.
8. Coates JT, Sun S, Leshchiner I, Thimmiah N, Martin EE, McLoughlin D, Danysh BP, Slowik K, Jacobs RA, Rhrissorrakrai K, *et al*: Parallel genomic alterations of antigen and payload targets mediate polyclonal acquired clinical resistance to sacituzumab govitecan in triple-negative breast cancer. Cancer Discov 11: 2436-2445, 2021.
9. Goodman CR, Seagle BL, Friedl TWP, Rack B, Lato K, Fink V, Cristofanilli M, Donnelly ED, Janni W, Shahabi S and Strauss JB: Association of circulating tumor cell status with benefit of radiotherapy and survival in early-stage breast cancer. JAMA Oncol 4: e180163, 2018.
10. Alamilla-Presuel JC, Burgos-Molina AM, González-Vidal A, Sendra-Portero F and Ruiz-Gómez MJ: Factors and molecular mechanisms of radiation resistance in cancer cells. Int J Radiat Biol 98: 1301-1315, 2022.
11. Zhao W, Sun M, Li S, Chen Z and Geng D: Transcription factor ATF3 mediates the radioresistance of breast cancer. J Cell Mol Med 22: 4664-4675, 2018.
12. Troschel FM, Böhly N, Borrmann K, Braun T, Schwickert A, Kiesel L, Eich HT, Götte M and Greve B: miR-142-3p attenuates breast cancer stem cell characteristics and decreases radioresistance in vitro. Tumour Biol 40: 1010428318791887, 2018.
13. Perez-Añorve IX, Gonzalez-De la Rosa CH, Soto-Reyes E, Beltran-Anaya FO, Del Moral-Hernandez O, Salgado-Albarran M, Angeles-Zaragoza O, Gonzalez-Barrios JA, Landero-Huerta DA, Chavez-Saldaña M, *et al*: New insights into radioresistance in breast cancer identify a dual function of miR-122 as a tumor suppressor and oncomiR. Mol Oncol 13: 1249-1267, 2019.
14. Feketea G, Bocsan CI, Popescu C, Gaman M, Stanciu LA and Zdrenghea MT: A review of macrophage MicroRNAs' role in human asthma. Cells 8: 42, 2019.
15. Xue T, Liang W, Li Y, Sun Y, Xiang Y, Zhang Y, Dai Z, Duo Y, Wu L, Qi K, *et al*: Ultrasensitive detection of miRNA with an antimonene-based surface plasmon resonance sensor. Nat Commun 10: 28, 2019.
16. Ni Q, Stevic I, Pan C, Müller V, Oliveira-Ferrer L, Pantel K and Schwarzenbach H: Different signatures of miR-16, miR-30b and miR-93 in exosomes from breast cancer and DCIS patients. Sci Rep 8: 12974, 2018.
17. Pan C, Sun G, Sha M, Wang P, Gu Y and Ni Q: Investigation of miR-93-5p and its effect on the radiosensitivity of breast cancer. Cell Cycle 20: 1173-1180, 2021.
18. Livak KJ and Schmittgen TD: Analysis of relative gene expression data using real-time quantitative PCR and the 2(-Delta Delta C(T)) method. Methods 25: 402-408, 2001.
19. Amin MB, Edge S, Greene F, Byrd DR, Brookland RK, Washington MK, Gershenwald JE, Compton CC, Hess KR, Sullivan DC, *et al* (eds): AJCC cancer staging manual. 8th edition. Springer International Publishing, New York, NY, 2017.
20. Tajbakhsh A, Rivandi M, Abedini S, Pasdar A and Sahebkar A: Regulators and mechanisms of anoikis in triple-negative breast cancer (TNBC): A review. Crit Rev Oncol Hematol 140: 17-27, 2019.
21. Fultang N, Illendula A, Chen B, Wu C, Jonnalagadda S, Baird N, Klase Z and Peethambaran B: Strictinin, a novel ROR1-inhibitor, represses triple negative breast cancer survival and migration via modulation of PI3K/AKT/GSK3ß activity. PLoS One 14: e217789, 2019.
22. Ahmed K, Koval A, Xu J, Bodmer A and Katanaev VL: Towards the first targeted therapy for triple-negative breast cancer: Repositioning of clofazimine as a chemotherapy-compatible selective Wnt pathway inhibitor. Cancer Lett 449: 45-55, 2019.
23. Sun XY, Han XM, Zhao XL, Cheng XM and Zhang Y: MiR-93-5p promotes cervical cancer progression by targeting THBS2/MMPS signal pathway. Eur Rev Med Pharmacol Sci 23: 5113-5121, 2019.
24. Wu H, Liu L and Zhu JM: MiR-93-5p inhibited proliferation and metastasis of glioma cells by targeting MMP2. Eur Rev Med Pharmacol Sci 23: 9517-9524, 2019.
25. Wang Q, Su C, Li J and Wei C: Mechanism of the enhancing effects of miR-93 on resistance of breast cancer MCF-7 cells to adriamycin. Oncol Lett 16: 3779-3783, 2018.
26. Ge YW, Liu ZQ, Sun ZY, Yu DG, Feng K, Zhu ZA and Mao YQ: Titanium particle-mediated osteoclastogenesis may be attenuated via bidirectional ephrin-B2/eph-B4 signaling *in vitro*. Int J Mol Med 42: 2031-2041, 2018.
27. Chen R, Yang X, Zhang B, Wang S, Bao S, Gu Y and Li S: EphA4 negatively regulates myelination by inhibiting schwann cell differentiation in the peripheral nervous system. Front Neurosci 13: 1191, 2019.
28. Pan Y, Lu S, Lei L, Lamberto I, Wang Y, Pasquale EB and Wang Y: Genetically encoded FRET biosensor for visualizing EphA4 activity in different compartments of the plasma membrane. ACS Sens 4: 294-300, 2019.
29. Okyere B, Mills WR, Wang X, Chen M, Chen J, Hazy A, Qian Y, Matson JB and Theus MH: EphA4/Tie2 crosstalk regulates leptomeningeal collateral remodeling following ischemic stroke. J Clin Invest 130: 1024-1035, 2020.
30. Chen X, Yang H, Zhou X, Zhang L and Lu X: MiR-93 targeting EphA4 promotes neurite outgrowth from spinal cord neurons. J Mol Neurosci 58: 517-524, 2016.
31. Kina S, Kinjo T, Liang F, Nakasone T, Yamamoto H and Arasaki A: Targeting EphA4 abrogates intrinsic resistance to chemotherapy in well-differentiated cervical cancer cell line. Eur J Pharmacol 840: 70-78, 2018.
32. de Marcondes PG and Morgado-Diaz JA: The role of EphA4 signaling in radiation-induced EMT-like phenotype in colorectal cancer cells. J Cell Biochem 118: 442-445, 2017.
33. de Marcondes PG, Bastos LG, De-Freitas-Junior JC, Rocha MR and Morgado-Díaz JA: EphA4-mediated signaling regulates the aggressive phenotype of irradiation survivor colorectal cancer cells. Tumour Biol 37: 12411-12422, 2016.
34. Sun Y, Qian J, Lu M and Xu H: Lower and reduced expression of EphA4 is associated with advanced TNM stage, lymph node metastasis, and poor survival in breast carcinoma. Pathol Int 66: 506-510, 2016.
35. Dong Y, Liu Y, Jiang A, Li R, Yin M and Wang Y: MicroRNA-335 suppresses the proliferation, migration, and invasion of breast cancer cells by targeting EphA4. Mol Cell Biochem 439: 95-104, 2018.
36. Zheng J, Wang B, Zheng R, Zhang J, Huang C, Zheng R, Huang Z, Qiu W, Liu M, Yang K, *et al*: Linc-RA1 inhibits autophagy and promotes radioresistance by preventing H2Bub1/USP44 combination in glioma cells. Cell Death Dis 11: 758, 2020.
37. Sen R and Baltimore D: Multiple nuclear factors interact with the immunoglobulin enhancer sequences. Cell 1986. 46: 705-716. J Immunol 177: 7485-7496, 2006.
38. Hou Y, Liang H, Rao E, Zheng W, Huang X, Deng L, Zhang Y, Yu X, Xu M, Mauceri H, *et al*: Non-canonical NF-κB antagonizes STING sensor-mediated DNA sensing in radiotherapy. Immunity 49: 490-503.e4, 2018.
39. Lu H, Clauser KR, Tam WL, Fröse J, Ye X, Eaton EN, Reinhardt F, Donnenberg VS, Bhargava R, Carr SA and Weinberg RA: A breast cancer stem cell niche supported by juxtacrine signalling from monocytes and macrophages. Nat Cell Biol 16: 1105-1117, 2014.